The Astrophysical Journal Letters, 898:L55 (6pp), 2020 August 1 https://doi.org/10.3847/2041-8213/aba83c

FRB 200428: An Impact between an Asteroid and a Magnetar

Jin-Jun Geng[1,2], Bing Li[3,4], Long-Biao Li[5,6], Shao-Lin Xiong[3], Rolf Kuiper[2], and Yong-Feng Huang[1,6]
[1] School of Astronomy and Space Science, Nanjing University, Nanjing 210023, People's Republic of China; gengjinjun@nju.edu.cn
[2] Institute of Astronomy and Astrophysics, University of Tübingen, Auf der Morgenstelle 10, D-72076,Tübingen, Germany
[3] Key Laboratory of Particle Astrophysics, Institute of High Energy Physics, Chinese Academy of Sciences, Beijing 100049, People's Republic of China; libing@ihep.ac.cn
[4] Particle Astrophysics Division, Institute of High Energy Physics, Chinese Academy of Sciences, Beijing 100049, People's Republic of China
[5] School of Mathematics and Physics, Hebei University of Engineering, Handan 056005, People's Republic of China
[6] Key Laboratory of Modern Astronomy and Astrophysics (Nanjing University), Ministry of Education, Nanjing 210023, People's Republic of China
Received 2020 June 13; revised 2020 July 20; accepted 2020 July 22; published 2020 August 4

Abstract

A fast radio burst (FRB) was recently detected to be associated with a hard X-ray burst from the Galactic magnetar SGR 1935+2154. Scenarios involving magnetars for FRBs are hence highly favored. In this work, we suggest that the impact between an asteroid and a magnetar could explain such a detection. According to our calculations, an asteroid of mass 10^{20} g will be disrupted at a distance of 7×10^9 cm when approaching the magnetar. The accreted material will flow along the magnetic field lines from the Alfvén radius $\sim 10^7$ cm. After falling onto the magnetar's surface, an instant accretion column will be formed, producing a Comptonized X-ray burst and an FRB in the magnetosphere. We show that all the observational features of FRB 200428 could be interpreted self-consistently in this scenario. We predict quasi-periodic oscillations in this specific X-ray burst, which can serve as an independent observational test.

Unified Astronomy Thesaurus concepts: Minor planets (1065); Pulsars (1306); Radio pulsars (1353); Magnetars (992); Soft gamma-ray repeaters (1471); Astronomical radiation sources (89); Burst astrophysics (187); Non-thermal radiation sources (1119); Neutron stars (1108); Radio bursts (1339)

1. Introduction

The physical origin of fast radio bursts (FRBs) has long remained mysterious. Their high dispersion measures indicate an extragalactic origin in the past years, and the corresponding isotropic energy released is then 10^{39-40} erg. Many catastrophic models like compact object mergers/interactions, the collapse of compact objects, or giant flares/pulses in magnetars, etc. are proposed to explain FRBs (see Platts et al. 2019 for a living review of these models). The observational data of FRBs are quickly growing thanks to the efforts of many telescopes (e.g., Canadian Hydrogen Intensity Mapping Experiment, or CHIME). The first FRB was discovered by Lorimer et al. (2007). As the number of FRBs increased, it was found that some of them are individual events, i.e., do not repeat within a monitor period. On the other hand, some sources have been repeating since discovery (The CHIME/FRB Collaboration et al. 2019). The repeating FRB 121102 has been bursting in a seemingly irregular/cluster[7] pattern for over 7 yr (Spitler et al. 2016). In addition, the repeating FRB 180916.J0158+65 shows ~16 day periodic activity (The CHIME/FRB Collaboration et al. 2020a), which strongly implies the source is modulated by the orbital motion of a binary system. It is still uncertain whether repeating or "non-repeating" is due to observational bias, e.g., we are not in the most active window for the individual FRB, or different astrophysical origin sources (Palaniswamy et al. 2018; Li et al. 2019).

Recently, an FRB has been reported to be spatially coincident with the galactic soft gamma-ray repeater (SGR) 1935+2154 (Bochenek et al. 2020; Lin et al. 2020b; The CHIME/FRB Collaboration et al. 2020b), also associated with a hard X-ray burst detected by several instruments including the INTErnational Gamma-Ray Astrophysics Laboratory (INTEGRAL; Mereghetti et al. 2020), the Hard X-ray Modulation Telescope (Insight-HXMT; Li et al. 2020), the Astro-rivelatore Gamma a Immagini LEggero (AGILE; Tavani et al. 2020), the Neutron star Interior Composition Explorer (NICER; Pearlman et al. 2020), and Konus-Wind (Ridnaia et al. 2020). Although this FRB (FRB 200428 hereafter) is ~25 times less energetic than the weakest FRB previously detected from cosmological FRB sources, the association of FRB 200428 with SGR 1935+2154 supports the idea that the magnetar scenario should work for at least some FRBs. However, detailed analyses indicate that a single magnetar model is very difficult to account for the observational properties of all FRBs (Margalit et al. 2020). Therefore, several models may be expected for FRBs, which invoke authors to refine their specific models to address corresponding characteristics and predictions (e.g., Lu et al. 2020).

It has been proposed that small solid bodies such as asteroids or comets can occasionally impact neutron stars (NSs), which may trigger the energy release in the NS magnetosphere (Colgate & Petschek 1981; Huang & Geng 2014) and hence FRBs (Geng & Huang 2015). Within this scenario, the predicted X-ray radiation from heated crust after the collision is generally too faint to be detected at the cosmological distance. Dai et al. (2016) studied the electron acceleration mechanism during the collision process in great detail, and suggested that the repeatability of FRB 121102 can be explained as due to multiple asteroid collision events. Very recently, Dai (2020) argued that the observational features of FRB 200428 and its associated X-ray burst can be well explained by the magnetar–asteroid collision model. In particular, he suggested that the two pulses of FRB 200428 are produced when two major iron–nickel fragments of the

[7] Rajwade et al. (2020) reported a detection of tentative periodic behavior of FRB 121102 over the span of five years of data, which invokes further follow-up observations to affirm.

disrupted asteroid cross the magnetic lines around the Alfvén radius. Here, we further study the interaction between the asteroids and the NSs by focusing on the formation of the instant accretion column and the consequent emissions. The association of galactic FRB 200428 with a ~10 ms X-ray burst motivates us to test our scenario, especially in the framework of the magnetar, which has much stronger magnetic fields.

The structure of this Letter is as follows. We describe the interaction processes in Section 2. In Section 3, we calculate the resulting emission from the interaction. Finally, in Section 4, we discuss the implication of our model and summarize our conclusions.

2. Magnetar–Asteroid Interaction

SGR 1935+2154 is a magnetar with rotational period $P = 3.24$ s (Stamatikos et al. 2014) and a surface dipolar magnetic field $B_{\rm NS} \simeq 2.2 \times 10^{14}$ G derived from the spin-down rate $\dot{P} \simeq 1.43 \times 10^{-11}\,{\rm s\,s^{-1}}$ (Israel et al. 2016). It is associated with the supernova remnant (SNR) G57.2+0.8 (Gaensler 2014), of which the distance is roughly within a range of 6–15 kpc (Sun et al. 2011; Pavlović et al. 2013; Kothes et al. 2018; Zhong et al. 2020; Zhou et al. 2020). In this work, we adopt $D_L = 10$ kpc for SGR 1935+2154, and the uncertainty of D_L will not affect our results significantly. This magnetar has exhibited multiple episodes of outbursts since discovery (Lin et al. 2020a).

When an asteroid approaches a magnetar of mass $M_{\rm NS}$, it will be tidally disrupted due to gravity. For an Fe–Ni asteroid with a mass $m_{\rm a}$, density $\rho_{\rm a}$, radius $r_{\rm a}$, and shear strength s, its breakup radius is (Colgate & Petschek 1981)

$$R_b = (\rho_{\rm a} r_{\rm a}^2 M_{\rm NS} G/s)^{1/3} = 6.8 \times 10^9 m_{\rm a,20}^{2/9} \rho_{\rm a,0.9}^{1/9} s_{10}^{-1/3} M_{\rm NS,1.4M_\odot}^{1/3}\ {\rm cm}, \quad (1)$$

where G is the gravitational constant. The convention $Q_x = Q/10^x$ in cgs units is adopted hereafter. The light cylinder of the magnetar is

$$R_{\rm LC} = c/\Omega = 1.5 \times 10^{10}\,{\rm cm}, \quad (2)$$

where $\Omega = 2\pi/P$ is the angular velocity of the magnetar. Since $R_b \leqslant R_{\rm LC}$, the disruption of the asteroid starts roughly within the magnetosphere. As the asteroid material gets much closer to the magnetar, the magnetic field begins to disturb the inflow at the so-called Alfvén radius $R_{\rm A}$. The equilibrium of kinetic and magnetic energy

$$\rho_{\rm a} \frac{v_{\rm ff}(R_{\rm A})^2}{2} = \frac{B^2(R_{\rm A})}{8\pi} \quad (3)$$

gives the Alfvén radius

$$R_{\rm A} = 1.1 \times 10^7 B_{\rm NS,14}^{2/5} R_{\rm NS,6}^{6/5} \rho_{\rm a,0.9}^{-1/5} M_{\rm NS,1.4M_\odot}^{-1/5}\ {\rm cm}, \quad (4)$$

where $v_{\rm ff}$ is the freefall velocity, $R_{\rm NS}$ is the radius of the magnetar, and a dipole magnetic field $B \propto R^{-3}$ is adopted. Within the Alfvén radius we expect that the matter will flow along field lines. The difference of arrival time at the magnetar surface for the leading and lagging fragments is $\sim 10\, m_{\rm a,20}^{4/9} s_{10}^{-1/6} \rho_{\rm a,0.9}^{-5/18} M_{\rm NS,1.4M_\odot}^{-1/3}$ ms (Geng & Huang 2015), which is less than the active duration of the radio/X-ray burst.

It should be noted that the magnetar–asteroid interaction above requires a relatively low magnetar surface temperature to avoid the evaporation of the asteroid (see details in Cordes & Shannon 2008) before its breakup. The NS surface temperature is likely to be 10^5–10^6 K in the literature but remains very uncertain. Considering the age of the SNR G57.2+0.8 hosting the magnetar SGR 1935+2154 is $\geqslant 2 \times 10^4$ yr (Zhou et al. 2020), the magnetar surface temperature could be $\leqslant 10^{5.4}$ K for a magnetar mass of $\geqslant 1.5\,M_\odot$ because cooling is much more efficient for high-mass NSs (Harding & Lai 2006). Such a surface temperature could ensure that the asteroid temperature in thermal equilibrium with the magnetar surface radiation (-Cordes & Shannon 2008) is below the iron evaporation point of about 2000 K at R_b. Therefore, our scenario favors the association of FRBs with relatively old and massive NSs.

Nonthermal radiation from the magnetar, i.e., the low-frequency Poynting flux-dominated flow close to the star and the flux of X-rays and gamma-rays associated with pair creation farther out (Kirk et al. 2009), may also cause the evaporation of the asteroid. For the low-frequency Poynting flux-dominated flow from the magnetar, since the ratio of the size of the body to the incident wavelength is $r_{\rm a}/(cP) = 2 \times 10^{-5} \ll 1$, the corresponding evaporation should be negligible according to the Mie theory (Kotera et al. 2016). Heating by high-energy particles may evaporate an orbiting asteroid at a close distance from the magnetar. However, since the asteroid is falling and the fraction of particles' kinetic energy in the pulsar's energy outflowing is decreasing when moving closer to the magnetar, the asteroid would have not enough time to evaporate completely. So heating by the nonthermal radiation from the magnetar also will not significantly affect our conclusion.

2.1. X-Ray Burst

Similar to the accretion of matter onto a compact object in binary systems, an *instant accretion column* will form in our scenario (see Figure 1). As the accreting matter flows along magnetic field lines to the polar cap, it will become highly supersonic and essentially in freefall. Before landing on the magnetar's surface, since the infalling material needs to be decelerated to subsonic, some sort of strong shock must occur in the accretion stream. After the shock, the hot gas settles to the NS surface in the magnetically confined column. Since our understanding of the column structure/shock characteristics is far from complete, here, we adopt a simple model to estimate basic parameters for the instant accretion column.

The isotropic fluence of the X-ray burst is $\sim 7 \times 10^{-7}\,{\rm erg\,cm^{-2}}$, lasting for $\delta t \sim 150$ ms. We attribute the X-ray burst energy to the release of gravitational potential energy of the asteroid, i.e.,

$$E_X = \eta \frac{G M_{\rm NS} m_{\rm a}}{R_{\rm NS}}, \quad (5)$$

where η is the efficiency of energy transforming. Taking $E_X = 8 \times 10^{39}$ erg and typical $\eta \sim 0.1$, the asteroid mass needed is $m_{\rm a} = 4 \times 10^{20}$ g. This mass is roughly in the mass range of normal asteroids. The average X-ray luminosity is $L_{\rm X} = E_X/\delta t = 5 \times 10^{40}\,{\rm erg\,s^{-1}}$, and the corresponding accretion rate is $\dot{M} = m_{\rm a}/\delta t = 2.7 \times 10^{21}\ {\rm g\,s^{-1}}$. The X-ray luminosity of the burst exceeds the Eddington luminosity ($L_{\rm Edd} \approx 2 \times 10^{38} M_{\rm NS,1.4\,M_\odot}\ {\rm erg\,s^{-1}}$), indicating the column is radiatively dominated. Due to the increasing magnetic pressure approaching the magnetar surface, at the magnetar's surface,

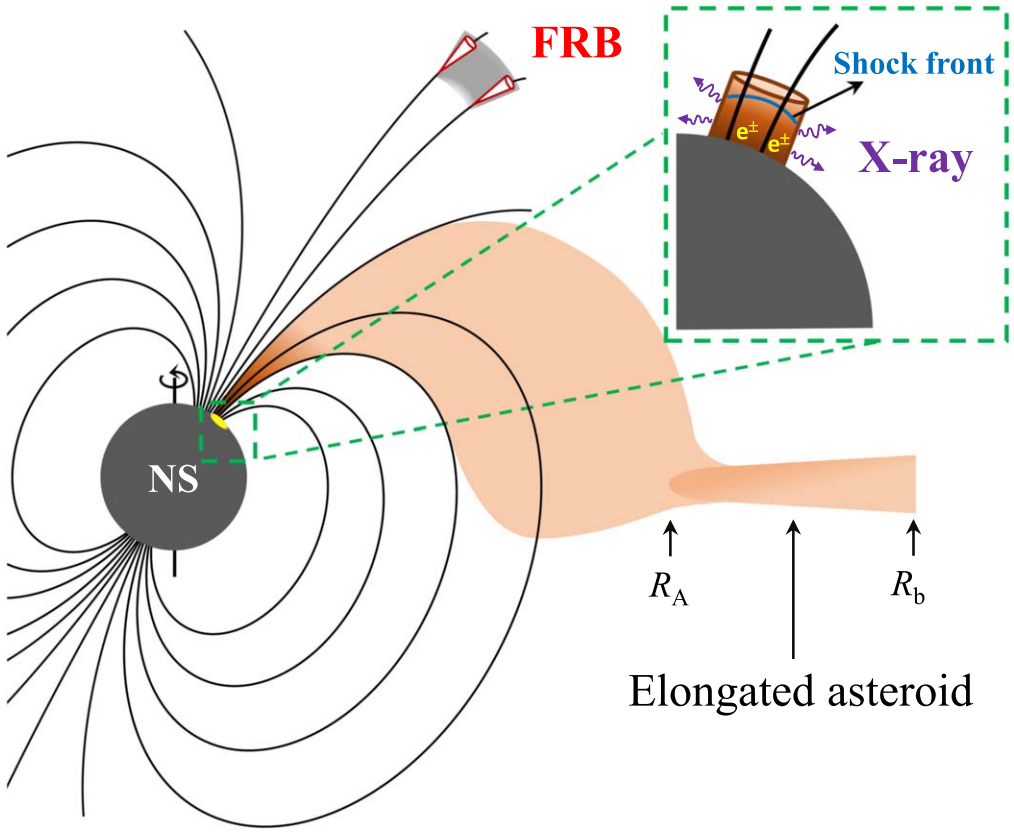

Figure 1. Schematic illustration of the impact between an asteroid and a magnetar. The asteroid gets elongated after entering R_b and further accreted along field lines within R_A. An instant accretion column is formed after collision onto the magnetar surface, producing a Comptonized X-ray burst and an FRB in the magnetosphere.

we assume that the cross-section of the accretion column is a thin rectangle of width d and length l. The polar angle (with respect to the magnetic axis) of this rectangle could be estimated by the landing point of accreted material, i.e., $\theta_{\rm land} = \arcsin(\sqrt{R_{\rm NS}/R_{\rm A}})$. Then l could be estimated as $l \approx 2\pi R_{\rm NS}\sin\theta_{\rm land} \times \delta t/P = 8 \times 10^4$ cm. The freefall velocity at the surface is $v_{\rm ff} = \sqrt{2GM_{\rm NS}/R_{\rm NS}}$. After the shock, the plasma falls down to a velocity of $v_{\rm fd} = v_{\rm ff}/7$ (Lyubarskii & Syunyaev 1982; Becker 1998) and the mass density changes as $\rho_{\rm ps} = \dot{M}/(ldv_{\rm fd})$.

Following the calculations of Mushtukov et al. (2015), the height of the accretion column H can be estimated from

$$L_X \approx 7.6\left(\frac{l/d}{10}\right)\frac{\kappa_{\rm T}}{\kappa_\perp} f\left(\frac{H}{R_{\rm NS}}\right) L_{\rm Edd}, \tag{6}$$

where $f\left(\frac{H}{R_{\rm NS}}\right) = \ln\left(1+\frac{H}{R_{\rm NS}}\right) - \frac{H}{R_{\rm NS}+H}$, $\kappa_{\rm T}$ is the Thomson electron scattering opacity of the solar mix plasma (the mean number of nucleons per electron is 1.17), and $\kappa_\perp$ is the opacity across the field lines. For a strong magnetic field and a typical photon energy E_γ (~84 keV for this burst) less than cyclotron energy $E_{\rm cycl}$, $\kappa_{\rm T}/\kappa_\perp \sim (E_\gamma/E_{\rm cycl})^{-2} \sim 1000$ (Canuto et al. 1971). We assume thermodynamical equilibrium deep inside the column and the plasma temperature to be T; the radiation field energy density in the deep center could be written as

$$P_{\rm rad} \approx \rho_{\rm ps}\frac{GM_{\rm NS}}{R_{\rm NS}+H}\frac{H}{R_{\rm NS}} \approx \frac{aT^4}{3}, \tag{7}$$

where a is the radiation constant. An empiric value of $l/d \sim 10$–100 is usually adopted in previous studies (Basko & Sunyaev 1976; Mushtukov et al. 2015). We find that our scenario could well explain the spectral feature of the X-rays if we chose $d = l/10 = 8 \times 10^3$ cm. Taking $L_{\rm X} = 5 \times 10^{40}$ erg s^{-1}, we obtain $H/R_{\rm NS} = 0.3$, $T \approx 2 \times 10^9$ K, or $kT \approx 170$ keV (k is the Boltzmann constant). On the other hand, the effective temperature ($T_\perp$) corresponding to the escaping flux (perpendicular to the field lines) is determined by the emergent flux

$$F_{\perp,\rm esp} \approx \frac{4cP_{\rm rad}}{\rho_{\rm ps}\kappa_\perp d} = \sigma_{\rm SB}T_\perp^4, \tag{8}$$

where $\sigma_{\rm SB}$ is the Stefan–Boltzmann constant. This relation gives $kT_\perp \approx 40$ keV, roughly consistent with the cutoff energy ~80 keV of the X-ray burst (Li et al. 2020).

More detailed processes should be considered for the radiation from the spot. High temperatures of the column result in the creation of electron–positron pairs, so that soft X-ray photons will be bulk Comptonized by e^+e^- pair plasmas before escaping. The pair number density could be given by (Mushtukov et al. 2019)

$$n_\pm \simeq 1.8 \times 10^{30} e^{-m_e c^2/kT}\left(\frac{kT}{m_e c^2}\right)^{3/2} {\rm cm}^{-3}, \tag{9}$$

from which we get $n_\pm \simeq 3 \times 10^{28}\,{\rm cm}^{-3}$ using $kT = 170$ keV. Considering the total energy of accreting material is going into pair creation, the Lorentz factor of the pairs $\gamma_\pm$ could be

obtained from

$$(\Gamma_{\rm ff} - \Gamma_{\rm fd})\rho_{\rm ps}c^2 = 2\gamma_{\pm}n_{-}m_e c^2, \quad (10)$$

where $\Gamma_{\rm ff/fd} = (1 - (v_{\rm ff/fd}/c)^2)^{-1/2}$, which gives $\gamma_{\pm} \simeq 8$. The scattering between the seed thermal/bremsstrahlung photons of $\sim$1 keV and e^+e^- pairs will result in a hard photon energy of 60 keV (Becker & Wolff 2007), which is also consistent with the cutoff energy of this X-ray burst. To obtain an accurate photon spectrum, we need to solve the Kompaneet's equation, which is beyond the scope of this work. Scattering, recoil and escaping from a finite medium should be included. However, according to studies of unsaturated Compton scattering in X-ray binaries, the emerging spectrum is expected to be a cutoff power-law shape (Ferrigno et al. 2016), which is consistent with the spectral feature of the X-ray burst here.

The X-ray burst showed two hard peaks with a separation of $\sim$30 ms. This could be understood by supposing that the elongated asteroid breaks into two main fragments around R_b (Dai 2020). We can infer that the distance between these two fragments should be roughly 3.5×10^6 cm, if we attribute the time separation of X-ray peaks to the difference of the arrival time of two fragments (using Equation (3) in Geng & Huang 2015). This distance is comparable with the radius of the asteroid before elongation, making the explanation more plausible.

2.2. Coherent Radio Pulse

FRB 200428 consists of two subbursts with durations of $\sim$0.6 ms and $\sim$0.34 ms, respectively, separated by $\sim$30 ms (The CHIME/FRB Collaboration et al. 2020b). For the first subburst, the primary beam detection from the Survey for Transient Astronomical Radio Emission 2 (STARE2) gives that its isotropic-equivalent luminosity is $L_{\rm FRB} = 4.2 \times 10^{38}$ erg s^{-1} at band $\sim$1.4 GHz (Bochenek et al. 2020). The second subburst is a bit fainter. Below, we will take the first subburst as the typical case in our interpretation.

It is still uncertain how coherent radio emission is produced from pulsars. Coherent mechanisms, either by charged bunches (e.g., Ruderman & Sutherland 1975; Benford & Buschauer 1977; Lyutikov et al. 2016; Yang & Zhang 2018; Kumar & Bošnjak 2020) or a maser mechanism (e.g., Blandford 1975; Luo & Melrose 1992; Lyubarsky 2014; Metzger et al. 2019) due to growth of plasma instabilities are proposed to produce radio emission. The same situation has also confronted us in the FRB. Since the time delay between the radio signal and the X-ray burst is in good agreement with the dispersion delay, both of them are suggested to originate within the magnetosphere, which motivates us to explain the radio pulse with curvature radiation from bunches.

As mentioned in the previous subsection, the landing of accretion material onto the NS surface produces abundant e^+e^- pairs. Considering that the landing point of the column $\theta_{\rm land}$ is beyond the gap region of the NS, only a small portion of these pairs will flow into the gap region. On the other hand, the large electric field in the gap can accelerate electrons and produce pair cascade within a very short timescale $\sim$1 μs (Mitra 2017). During the rising phase of the X-ray burst, the arrival of the charges will screen the gap electric field due to the continuous increasing supply of charges. The screen is destructed once the charge density from the accretion column decreases to a threshold during the decline phase of the X-ray burst. At that time, these charges from the column will be accelerated (with Lorentz factors of γ) to flow along the open field lines. After the leaving of this plasma cloud, the discharge from the gap can initiate soon within a period of $\sim$1 μs, which produces a following plasma cloud. When it caught up with the plasma cloud emitted from accretion material, the overlapping of the slow- and fast-moving particles will lead to the two-stream instability in the plasma, hence the coherent emission. The height of the gap is (Mitra 2017)

$$h = 95 B_{\rm NS,14}^{-4/7} P^{1/7} \dot{P}_{-11}^{-2/7} R_{\rm NS,\,6}^{2/7}\ {\rm cm}. \quad (11)$$

The velocity difference between the slow- and fast-moving particles is about $\Delta v = c/(2\gamma^2)$, and the time for the particles to overlap is $h/\Delta v$. Hence, the instability can develop at a distance of $r_{\rm emi} \sim ch/\Delta v \simeq 2\gamma^2 h$ from the NS. The corresponding characteristic frequency of curvature emission is

$$\nu_c = \gamma^3 \frac{3c}{4\pi r_{\rm c}}, \quad (12)$$

where $r_{\rm c}$ is the curvature radius and is related to $r_{\rm emi}$ by $r_{\rm c} \simeq \frac{4r_{\rm emi}}{3\sin\theta_{\rm emi}}$ according to the magnetosphere geometry, and $\theta_{\rm emi}$ is the poloidal angle of the emission region. Therefore, we could obtain

$$\gamma = 677 \left(\frac{\nu_{\rm c}}{1.4\ {\rm GHz}}\right)\left(\frac{h}{65\ {\rm cm}}\right)\left(\frac{\sin\theta_{\rm emi}}{0.05}\right)^{-1}. \quad (13)$$

This is within the range of Lorentz factor (10^2–10^4) of e^+e^- accelerated from the NS gap.

Assuming the length of the bunching shell is Δ, the duration δt of the FRB pulse implies $\Delta \simeq c\delta t$. We further assume that the ratio of the shell's solid angle to 4π is f, then the emission volume is $V_{\rm emi} = 4\pi f r_{\rm emi}^2 \Delta$. Electrons radiate coherently in patches with a characteristic radial size of $\lambda = c/\nu_c$, and they can be casually connected in the relativistic beam of angle of $1/\gamma$; the corresponding volume of one small patch is $V_{\rm coh} = (4/\gamma^2) r_{\rm emi}^2 \lambda$. The number of the patches writes as $N_{\rm pat} \approx V_{\rm emi}/V_{\rm coh}$. Then the coherent curvature emission luminosity can be estimated as

$$L_{\rm coh} = (P_e N_{\rm coh}^2) \times N_{\rm pat}, \quad (14)$$

where $N_{\rm coh} = n_e \times V_{\rm coh}$ is the number of electrons in each patch. Using $L_{\rm coh} = fL_{\rm FRB}$, we can constrain the electron number density to be

$$n_e \simeq 4.6 \times 10^9 \left(\frac{L_{\rm FRB}}{4.2 \times 10^{38}\ {\rm erg\ s^{-1}}}\right)^{1/2}\left(\frac{\gamma}{677}\right)^{1/2} \times \left(\frac{r_{\rm emi}}{6 \times 10^7\ {\rm cm}}\right)^{-3/2}\left(\frac{\delta t}{0.6\ {\rm ms}}\right)^{-1/2}\left(\frac{\sin\theta_{\rm emi}}{0.05}\right)^{-1/2} \quad (15)$$

The corresponding plasma density near the NS surface should be $\sim n_e (r_{\rm NS}/r_{\rm emi})^{-2} \simeq 1.7 \times 10^{13}\,{\rm cm}^{-3}$. The Goldreich & Julian (1969) charge number density at the cap region is $n_{\rm GJ}(r_{NS}, \theta_{\rm open}) = 3.8 \times 10^{10}\,{\rm cm}^{-3}$, where $\sin\theta_{\rm open} = \sqrt{R_{\rm NS}/R_{\rm LC}}$. Therefore, a reasonable pair multiplicity factor of $\sim$400 is needed during the spark.

In our scenario, an FRB is emitted along open field lines at $r_{\rm emi} \sim 60\,R_{\rm NS}$, which indicates that the edge of the lightning cone of this magnetar may sweep the line of sight. Although the radiation position for the FRB and periodic radio pulsations

may be different, the detection of periodic radio pulsations may still be possible since we have little constraints on the f factor of the FRB. Interestingly, a $\sim 7\sigma$ detection of periodic radio pulsations from SGR 1935+2154 was reported very recently (Burgay et al. 2020). If such a detection is confirmed in the future, our scenario would be highly favored.

Usually, the direct collision between asteroids and the magnetar may be very rare since the recurrence time of such strong direct impacts ($m_a \geqslant 10^{18}$ g) in a typical NS planetary system can be as large as $\sim 10^6$–10^7 yr according to previous studies (Tremaine & Zytkow 1986; Litwin & Rosner 2001). However, in some special cases, it may still be possible that the NS is passing through an asteroid belt as suggested by Dai et al. (2016) so that several FRBs could be produced within a short period due to multiple collisions. A much weaker (30 mJy) radio pulse has been observed by the Five-hundred-meter Aperture Spherical radio telescope two days after the two FRB pulses (Zhang et al. 2020). It is doubtful if this weak burst can be regarded as an FRB or not because its equivalent isotropic energy is almost 10^8 times smaller than the two pulses. If it were really from SGR 1935+2154, it may be caused by pollution of NS magnetospheres by low-level accretion from a circumpulsar debris disk (Cordes & Shannon 2008).

2.3. Follow-up Burst

The landing of asteroid material onto the magnetar will increase the moment of inertia of the magnetar, leading to an abrupt change of rotational frequency of the magnetar (Huang & Geng 2014). Assuming the moment of inertia of the magnetar crust I_c is only 1% of the total moment of inertia, i.e., $I_c = 0.01 \times \frac{2}{5} M_{\rm NS} R_{\rm NS}^2 \sim 10^{43}\,{\rm g\,cm^2}$. The asteroid of mass 4×10^{20} g will lead to an instantaneous change in frequency $\Delta\nu \sim -1.0 \times 10^{-12}$ Hz, which is too small to be detected from X-ray/radio observation. However, we have ignored the orbital angular momentum of the asteroid itself in the above estimate. The transfer of the asteroid's orbital angular momentum to the magnetar crust could result in a $\Delta\nu$ of magnitude $\sim 10^{-8}$ Hz. Future observations of magnetars with radio pulses could help to identify this hypothesis.

The impact of the accretion column against the magnetar surface may also lead the crust to be more unstable, i.e., trigger the crustquakes (Thompson & Duncan 1995) or magnetic field line reconnection (Lyutikov 2003). This process heats the surface in one or more regions, from which seed thermal photons might be resonant cyclotron scattered by the electrons. As a result, an X-ray burst forest is expected to follow the FRB-associated X-ray burst. Since these following X-ray bursts come from the normal activities of an isolated magnetar, they are unlikely to be associated with further FRBs.

3. Summary and Discussion

We study the impact between an asteroid and a magnetar, trying to explain the association of the Galaxy FRB 200428 with an X-ray burst. For an asteroid with a mass of $\sim 10^{20}$ g falling onto the magnetar's surface, an instant accretion column will be formed, which produces a Comptonized X-ray burst and an FRB in the magnetosphere. Our calculations show that all the observational features could be self-consistently explained within this scenario.

Both the radio and the X-ray burst showed two peaks with a separation of ~ 30 ms. Similar substructures also exist in some extragalactic FRBs. This may be due to the unsmooth disruption process of the asteroid. At R_b, the asteroid may break into two or even more fragments (Dai 2020), making the later accretion flow and emission to be intermittent.

The accretion column in our scenario may be identified indirectly from the temporal variability of the burst. It is known that the postshock flow may be subject to a global thermal instability revealed by rapid variations of the cooling timescale with the shock speed. The instability drives the shock front to oscillate with respect to its stationary position, causing fluctuations in the emission flux (Saxton et al. 1998; Mignone 2005). This phenomenon has been detected in accreting white dwarfs, which show optical emission with quasi-periodic oscillations (QPOs) of ~several Hz (Imamura et al. 1991; Mouchet et al. 2017; Bera & Bhattacharya 2018). Unfortunately, radiative shocks in the accretion column onto magnetars are poorly studied in the literature, especially including the photon-e^+e^- pairs scattering processes. It is difficult for us to estimate the oscillating frequency within our current work. Nevertheless, the QPOs (if they exist) in the temporal variability of this X-ray burst from SGR 1935+2154 will strongly favor our scenario. At the same time, the QPO should emerge only in the burst associated with the FRB 200428, rather than the following bursts.

By now, the consensus on FRBs is that the radio emission of FRBs should be coherent. On the other hand, we are confident that coherent radio emission comes from the moving plasma cloud in the magnetosphere according to observations of pulsars. Therefore, what we have proposed belongs to processes that can trigger the coherent emission from the magnetosphere of NSs, resulting in a millisecond burst rather than normal pulsar pulses. It should be noted that multiple NS–asteroid impacts may produce repeating FRBs/periodic FRBs (see Dai et al. 2016; Dai & Zhong 2020 for details). Increasing observational constraints will help us to judge whether repeating FRBs have a unique or various origins in the future (Smallwood et al. 2019).

We thank the anonymous referee for valuable suggestions. We also thank Shuang-Nan Zhang, André Oliva, and Zi-Gao Dai for helpful discussions. This work is partially supported by the National Natural Science Foundation of China (grant Nos. 11903019, 11873030, 11833003, U1938201, and U1838113), and by the Strategic Priority Research Program of the Chinese Academy of Sciences ("multi-wave band Gravitational Wave Universe" grant Nos. XDB23040000, XDA15360300, and XDA15052700). R.K. acknowledges financial support via the Emmy Noether Research Group on Accretion Flows and Feedback in Realistic Models of Massive Star Formation funded by the German Research Foundation (DFG) under grant Nos. KU 2849/3-1 and KU 2849/3-2. L.B.L. acknowledges support from the Natural Science Foundation of Hebei Province of China (grant No. A2020402010).

ORCID iDs

Jin-Jun Geng https://orcid.org/0000-0001-9648-7295
Bing Li https://orcid.org/0000-0002-0238-834X
Long-Biao Li https://orcid.org/0000-0003-3098-9932
Rolf Kuiper https://orcid.org/0000-0003-2309-8963
Yong-Feng Huang https://orcid.org/0000-0001-7199-2906

References

Basko, M. M., & Sunyaev, R. A. 1976, MNRAS, 175, 395
Becker, P. A. 1998, ApJ, 498, 790
Becker, P. A., & Wolff, M. T. 2007, ApJ, 654, 435
Benford, G., & Buschauer, R. 1977, MNRAS, 179, 189
Bera, P., & Bhattacharya, D. 2018, MNRAS, 474, 1629
Blandford, R. D. 1975, MNRAS, 170, 551
Bochenek, C. D., Ravi, V., Belov, K. V., et al. 2020, arXiv:2005.10828
Burgay, M., et al. 2020, ATel, 13783, 1
Canuto, V., Lodenquai, J., & Ruderman, M. 1971, PhRvD, 3, 2303
Colgate, S. A., & Petschek, A. G. 1981, ApJ, 248, 771
Cordes, J. M., & Shannon, R. M. 2008, ApJ, 682, 1152
Dai, Z. G. 2020, ApJL, 897, L40
Dai, Z. G., Wang, J. S., Wu, X. F., et al. 2016, ApJ, 829, 27
Dai, Z. G., & Zhong, S. Q. 2020, ApJL, 895, L1
Ferrigno, C., Pjanka, P., Bozzo, E., et al. 2016, A&A, 593, A105
Gaensler, B. M. 2014, GCN, 16533, 1
Geng, J. J., & Huang, Y. F. 2015, ApJ, 809, 24
Goldreich, P., & Julian, W. H. 1969, ApJ, 157, 869
Harding, A. K., & Lai, D. 2006, RPPh, 69, 2631
Huang, Y. F., & Geng, J. J. 2014, ApJL, 782, L20
Imamura, J. N., Rashed, H., & Wolff, M. T. 1991, ApJ, 378, 665
Israel, G. L., Esposito, P., Rea, N., et al. 2016, MNRAS, 457, 3448
Kirk, J. G., Lyubarsky, Y., & Petri, J. 2009, in Neutron Stars and Pulsars, Astrophysics and Space Science Library, Vol. 357, ed. W. Becker (Berlin: Springer), 421
Kotera, K., Mottez, F., Voisin, G., et al. 2016, A&A, 592, A52
Kothes, R., Sun, X., Gaensler, B., et al. 2018, ApJ, 852, 54
Kumar, P., & Bošnjak, Ž 2020, MNRAS, 494, 2385
Li, C. K., Lin, L., Xiong, S. L., et al. 2020, arXiv:2005.11071
Li, Y., Zhang, B., Nagamine, K., et al. 2019, ApJL, 884, L26
Lin, L., Göğüş, E., Roberts, O. J., et al. 2020a, ApJ, 893, 156
Lin, L., Zhang, C. F., Wang, P., et al. 2020b, arXiv:2005.11479
Litwin, C., & Rosner, R. 2001, PhRvL, 86, 4745
Lorimer, D. R., Bailes, M., McLaughlin, M. A., et al. 2007, Sci, 318, 777
Lu, W., Kumar, P., & Zhang, B. 2020, arXiv:2005.06736
Luo, Q., & Melrose, D. B. 1992, MNRAS, 258, 616
Lyubarskii, Y. E., & Syunyaev, R. A. 1982, SvAL, 8, 330
Lyubarsky, Y. 2014, MNRAS, 442, L9
Lyutikov, M. 2003, MNRAS, 346, 540
Lyutikov, M., Burzawa, L., & Popov, S. B. 2016, MNRAS, 462, 941
Margalit, B., Beniamini, P., Sridhar, N., et al. 2020, arXiv:2005.05283
Mereghetti, S., Savchenko, V., Ferrigno, C., et al. 2020, arXiv:2005.06335
Metzger, B. D., Margalit, B., & Sironi, L. 2019, MNRAS, 485, 4091
Mignone, A. 2005, ApJ, 626, 373
Mitra, D. 2017, JApA, 38, 52
Mouchet, M., Bonnet-Bidaud, J.-M., van Box Som, L., et al. 2017, A&A, 600, A53
Mushtukov, A. A., Ognev, I. S., & Nagirner, D. I. 2019, MNRAS, 485, L131
Mushtukov, A. A., Suleimanov, V. F., Tsygankov, S. S., et al. 2015, MNRAS, 454, 2539
Palaniswamy, D., Li, Y., & Zhang, B. 2018, ApJL, 854, L12
Pavlović, M. Z., Urošević, D., Vukotić, B., et al. 2013, ApJS, 204, 4
Pearlman, A. B., Majid, W. A., Prince, T. A., et al. 2020, arXiv:2005.08410
Platts, E., Weltman, A., Walters, A., et al. 2019, PhR, 821, 1
Rajwade, K. M., Mickaliger, M. B., Stappers, B. W., et al. 2020, MNRAS, 495, 3551
Ridnaia, A., Svinkin, D., Frederiks, D., et al. 2020, arXiv:2005.11178
Ruderman, M. A., & Sutherland, P. G. 1975, ApJ, 196, 51
Saxton, C. J., Wu, K., Pongracic, H., et al. 1998, MNRAS, 299, 862
Smallwood, J. L., Martin, R. G., & Zhang, B. 2019, MNRAS, 485, 1367
Spitler, L. G., Scholz, P., Hessels, J. W. T., et al. 2016, Natur, 531, 202
Stamatikos, M., Malesani, D., Page, K. L., et al. 2014, GCN, 16520, 1
Sun, X. H., Reich, P., Reich, W., et al. 2011, A&A, 536, A83
The CHIME/FRB Collaboration, Amiri, M., Andersen, B. C., et al. 2020a, Natur, 582, 351
The CHIME/FRB Collaboration, Anderson, B. C., Bandura, K., et al. 2019, ApJL, 885, L24
The CHIME/FRB Collaboration, Andersen, B. C., Bandura, K. M., et al. 2020b, arXiv:2005.10324
Tavani, M., Casentini, C., Ursi, A., et al. 2020, arXiv:2005.12164
Thompson, C., & Duncan, R. C. 1995, MNRAS, 275, 255
Tremaine, S., & Zytkow, A. N. 1986, ApJ, 301, 155
Yang, Y.-P., & Zhang, B. 2018, ApJ, 868, 31
Zhang, C. F., Jiang, J. C., Men, Y. P., et al. 2020, ATel, 13699, 1
Zhong, S. Q., Dai, Z. G., Zhang, H. M., et al. 2020, ApJL, 898, L5
Zhou, P., Zhou, X., Chen, Y., et al. 2020, arXiv:2005.03517